Harmonic analysis of atomic vapor magnetization for *in situ* calibration of tri-axial time-dependent magnetic field

Giuseppe Bevilacqua and Valerio Biancalana*
DSFTA Università di Siena - Via Roma 56 - 53100 Siena, Italy

Yordanka Dancheva
DSFTA Università di Siena - Via Roma 56 - 53100 Siena, Italy and
Aerospazio Tecnologie S.r.l. - 53040 Rapolano Terme (SI), Italy

Alessandro Fregosi
CNR - Istituto Nazionale di Ottica - Via G. Moruzzi 1 - 56124 Pisa (Italy)
(Dated: April 24, 2024)

We introduce a methodology to calibrate *in situ* a set of coils generating bi- or tri-axial magnetic fields, at frequencies where a calibration performed in static condition would be inaccurate. The coil constants are determined in a two-step procedure. Considering the presence of a static and of a time-dependent field, firstly, the static one is oriented perpendicularly to the polarization plane of a time dependent one; secondly, the polarization of the latter is made accurately circular. The methodology uses harmonic analysis of one component of the magnetization of an atomic sample whose spins adiabatically follow the time-dependent field.

I. INTRODUCTION

The application of precisely assigned magnetic fields, with tailored spatial and temporal distribution is at the core of many precision experiments in modern physics and particularly in atomic laser spectroscopy and quantum optics [1, 2]. The generation of well controlled triaxial, time-dependent magnetic fields is of interest also for other application areas [3]. Solenoids, Helmholtz pairs and other specifically designed coil arrangements [4] are commonly used to achieve the desired field structure. Numerically controlled power supplies permit fine adjustments of the magnetic field components as well as the generation of custom-designed time-dependent magnetic fields.

In instances requiring a two- or three-dimensional time-dependent field, setting its Cartesian and Fourier components with precise amplitude and relative phase may have a paramount importance [1, 5, 6].

The construction and characterization of magnetic field generators may follow both *a priori* and *a posteriori* approaches. The former is based on designing the current distribution (coil shape, and current waveform) in view of producing the appropriate fields, on the basis of the Maxwell's laws. The *a posteriori* approach consists in measuring the actually produced field and to adjust its features with opportune additional coils or with opportune variations of the driving current(s). This second approach is often essential to improve the accuracy. In fact, the magnetic field generators are often surrounded by conducting materials or magnetic shields whose effects cannot be precisely taken into account in simulations or calculations.

Several kinds of sensors can be used to measure the actual field, each of them coming with its inherent degree of precision, accuracy, spatial and time resolution, robustness etc. The use of Hall-effect or fluxgate sensors is often a favorite choice for their practicality, simple structure and vector response [7, 8]. However, in some applications they are not sufficiently precise or are not compatible with existing constraints.

Laser spectroscopy with its unrivaled precision is an area of research that can require extreme accuracy in magnetic field control. At the same time, it enables the construction of very sensitive magnetic detectors, suitable for nicely performing such task.

As proposed by Breschi et al.[9], an elegant and effective way to control the field with the accuracy required in atomic spectroscopy experiments and with detectors easily fitting in the setup is based on using the atomic sample itself as magnetometric sensor. This approach takes advantage from the high performance of optically pumped magnetometers, and avoids constraint issues because the atomic sample is already available as a part (typically the core!) of the experimental setup. This idea is at the basis of the *in-situ* calibration procedures that have been reported by several researchers.

H.Zhang et al. [10] present a method to infer the coil constant (ratio between field and current) with a high precision by means of a high-performance hyperpolarized He magnetometer.

A similar calibration method is proposed by Yao et al. [11], who use a hybrid potassium-rubidium magnetometer, analyzing the magnetic resonance under varying (swept) magnetic fields.

Chen et al. [12] propose a coil calibration method based on the duration of a $\pi/2$ pulse, which is precisely determined by the maximization of the initial amplitude of the free-induction-decay signal. The latter is gener-

ated by free precessing spins in Xenon gas polarized by collisions with optically pumped Rb vapour. This choice eliminates systematic errors that are possibly introduced by the laser radiation.

Zhao et al. [13] use calibrated coils to obtain vector response from a self-oscillating rubidium optically-pumped magnetometer interrogated by far detuned (hence non-destructive) probe radiation. This approach has similarities with that proposed by G.Zhang et al. [14] using a forced (Bell and Bloom) magnetometer. In this case atoms are optically pumped by elliptically polarized radiation, which permits to achieve a vector response from the analysis of orientation and alignment dynamics.

More recently Wang et al. [15] proposed a coil calibration method applied to a spin-exchange-relaxation-free optically pumped magnetometer based on the dynamic (transient) response of such system upon application of sudden variation of magnetic field along the three orthogonal directions.

A calibration method based on magnetic induction detection with an accurately aligned pickup coil has been proposed by K.Zhang et al. [16] for Helmholtz coils operated in a frequency range from few tens to several hundreds Hz.

A general feature shared by all the above mentioned works is to reduce the field measurement to a current (more commonly a voltage) measurement through an opportune set of calibration factors to be calculated or measured. The current-field linear dependence makes indeed possible to indirectly monitor the field by measuring the voltage across an assigned resistor connected in series with the field-generating coil. Those calibration factors are typically determined under static or quasi-static conditions, but can be used also in the case of time-dependent field, under the hypothesis that the instantaneous field can be inferred from the corresponding instantaneous voltage drop on the series resistor.

The last assumption may be no longer valid in case of fast varying fields and currents. Indeed spurious phenomena (e.g. parasitic capacitance of cables and coils) can cause the measured current across the series resistor be different from that actually flowing in the coil, moreover unperceived eddy currents may be induced in the coil proximity. Thus the high frequency terms of the produced field may substantially differ, in amplitude and phase, from the corresponding terms inferred from the voltage drop measured on the monitor resistance [7].

In the recent years our research group has devoted a substantial effort to study the dynamics of atomic spins evolving in (or driven by) arbitrarily oriented time-dependent magnetic fields, with tailored sets of Fourier components applied along several spatial directions. In this research we have studied [17, 18] and applied [19] interesting features of phenomena commonly referred to as *magnetic dressing* [20], focusing on cases where the dressing field contains various Fourier and Cartesian components [6, 21]. These studies require an accurate control of the amplitude and phases of the magnetic field components applied to the atomic sample.

The core of the presented work is an innovative methodology aimed to achieve an accurate coil calibration over a broad frequency range, beyond the limit at which coil constants determined under static conditions become imprecise.

The proposed methodology makes use of a harmonic analysis of the signal that monitors one component of the atom polarization that evolves in the presence of a strong rotating field.

We consider a magnetic field that is ideally made by a time-dependent component that rotates on a plane and a static one oriented perpendicularly to that plane and our goal is to detect imperfections of such field structure, which may consist in non-perfect perpendicularity of the static field, and in elliptical polarization of the time-dependent one.

The developed procedure is correspondingly made of two steps. The first step is to orient the static field perpendicularly to the polarization plane of the rotating one. The second one serves to establish a circular polarization of the rotating field. This permits to identify and counteract possible spurious effects occurring at higher frequencies and affecting amplitudes and phases of different field components.

The atomic sample is optically interrogated, with polarimetric techniques previously developed for magnetometric measurements, in such a way to produce a signal proportional to one component of the macroscopic magnetization. Diverse harmonic components of that signal bring information about the mentioned field imperfections, thus an inherently *in-situ* calibration procedure is developed on the basis of Fourier analysis.

The presentation is organized as follows: in Sec.II we describe the experimental setup, in Sec.III we describe (demanding calculus details to an Appendix) the principle of operation of the methodology to control the relative orientation of the static and the time-dependent fields and to refine the relative phases and amplitudes of the time-dependent field components. Demonstrative results are reported and analyzed in the Sec.IV. A synthesis of the achievements is drawn and shortly discussed in Sec.V.

II.   SETUP

The setup built to prepare and interrogate the atomic magnetization is described in Ref.[22], where it was used for magnetometric measurements. Briefly, Cs atoms are pumped by means of circularly polarized radiation tuned to the D1 line and probed with a weak linearly polarized radiation detuned by few GHz from the D2 line. A balanced polarimeter is used to measure the Faraday rotation of the probe polarization plane, which provides a signal proportional to the sample magnetization component along the probe-beam axis: this is the signal to be analyzed for our methodology. The two beams co-

propagate along the x direction and in magnetometric application a static field is applied along the z direction. The balanced polarimeter uses a transimpedance amplifier with a bandwidth of several kHz, enabling the detection of signals with a spectrum in the audio range.

The experiment is run in an unshielded environment, where the magnetic field and its first-order gradients are compensated by three large-size (180 cm) Helmholtz pairs and five quadrupole sources, all of them driven by numerically controlled current generators that can be set manually or automatically [23]. When needed, one of the field components is compensated partially to establish a static field.

Additional coils enable the application of time-dependent fields along the three directions. The co-propagating arrangement of the pump- and probe-beams permits the use of a solenoid for the x component, while the y and z components are generated by small size (45 cm and 50 cm size, respectively) squared Helmholtz pairs, each with 50 turns per coil. These three alternating field coils are supplied via audio-amplifiers that amplify three arbitrary waveforms generated by a digital-to-analog (DAC) converters card (NI 6343), as sketched in Fig.1. Depending on the required frequencies, matching series-impedances can be applied to improve the coupling between each amplifier and the respective coil. The current actually flowing in each coil is monitored by recording the voltage drop over series resistors, using analog-to-digital converters (ADC) available in the same NI-6343 card.
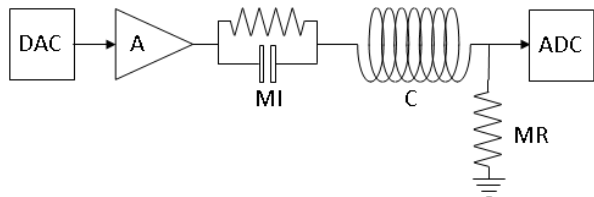

FIG. 1. Schematics of the time-dependent field generator and monitor for one Cartesian component of the time dependent field: DAC: digital-to-analog converter, programmed for arbitrary waveform generation; A: amplifier; MI: matching impedance; C: coil (solenoid or Helmholtz pair); MR: monitor resistance; ADC: analog to digital converter.

From the size, shape and number of turns in each coil it is possible to evaluate *a priori* the current-field calibration factor on the basis of basic equations, such as Biot-Savart and Ampère laws.

An *a posteriori* calibration is then performed, under static conditions, with the help of the magnetometer, by measuring the variations of the Larmor frequency in response to changes of the current flowing in the coils. The Larmor frequency can be evaluated scanning the frequency of the pump modulation across the magnetic resonance as described in [22] or estimating the frequency of a free precession signal as described, e.g., in [24, 25].

In the case of free-precession measurement, the procedure implemented for our setup is as follows: the pump laser is tuned to the $F_g = 3 \rightarrow F_e = 4$ D1 transition for 100 ms, then is abruptly blue-detuned by about 30 GHz by reducing its drive current. As soon as the pump radiation is made off-resonant, the data acquisition starts, lasting other 100 ms as to measure the transient signal produced by the free precession of the atomic spins.
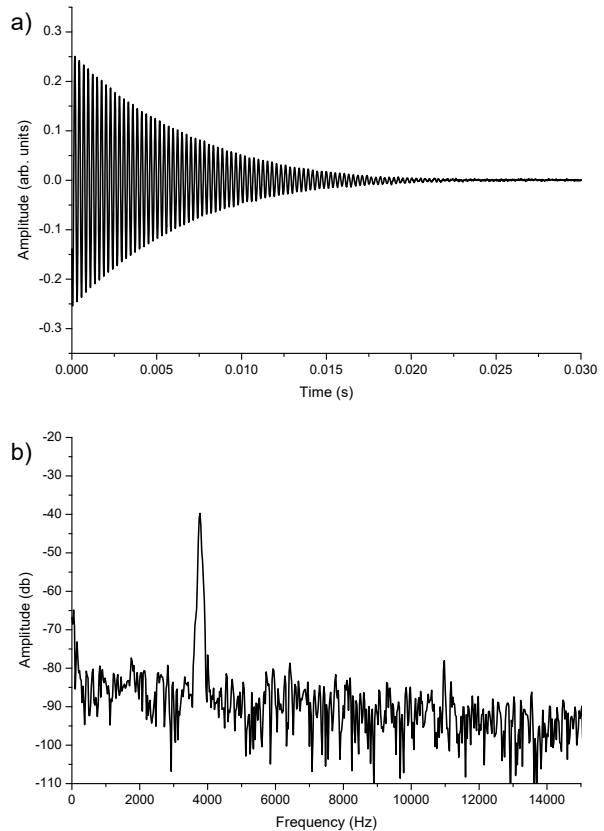

FIG. 2. Free precession signal in the time (a) and the frequency (b) domains.

An example of such transient signal is reported in Fig.2. No appreciable harmonic distortion is caused at the photo-detection stage: no harmonic peaks emerge from the noise floor, indicating that they are more than 45 dB weaker than the fundamental tone. The localization of the fundamental tone peak in Fig.2b permits to evaluate the static field. In this case the magnetic field is estimated to be $1.071 \mu\text{T} \pm 3\text{nT}$. A consistent value ($1.070 \mu\text{T} \pm 3\text{nT}$) was obtained from the analysis of the resonance profile obtained in forced conditions, i.e. running the magnetometer in the Bell and Bloom configuration [22]. The $\pm 3\text{nT}$ uncertainties are estimated from the standard deviation over large measurement sets, and they are due to the ambient field fluctuations.

As a starting point, the generation of the time-dependent field from each coil uses the calibration factors determined under static conditions. To this aim, the DAC is programmed to generate a signal with known

amplitude and phase at the desired frequency; this signal is amplified and applied to the coil; the voltage drop on the monitor resistor is acquired and analyzed to extract its phase and amplitude; the latter is then converted to current and then to field on the basis of the monitor resistance and the static coil constant; finally the DAC output is scaled and rephased to achieve the field settings (phase and amplitude) set by the operator. Being DAC and ADC of the diverse coils synchronous, this procedure enables the generation of field components with relative phase and amplitudes assigned on the basis of the static calibration factors.

Transient signal measurements are also applied to characterize time-dependent, three-dimensional magnetic fields, i.e. for the dynamic calibration procedure at the focus of the present work. In this case the signal is not due to a free precession of the spins around a static field, but to their strongly driven dynamics. The latter consists in an adiabatic following of the applied time-dependent field, as discussed in the following (Sec.III). The recorded signal consists of a damped oscillation as in the case of free induction decay measurement, but here the oscillation frequency is that of the rotating field.

III. METHODOLOGY

Our aim is an accurate determination of the coil constants for two orthogonal field generators, taking into account the amplitude and phase deviations that occur when the frequency of the field to be generated is too high, such as to make the constants determined in static conditions imprecise. To this aim, we generate a rotating field with a nominally circular polarization, using the static constants; we evaluate its actual ellipticity; and we eventually determine the corrections needed to compensate the detected discrepancies.

The idea at the basis of the proposed methodology relies on the adiabatic precession of the atomic sample magnetization around the instantaneous magnetic field to be characterized. The atomic spins follow adiabatically the time-dependent field under the condition that the instantaneous precession is much faster than the reorientation of the field. In other terms, with a time dependent field that rotates at an angular speed ω, it is required that

$$\gamma B \gg \omega, \tag{1}$$

where γ is the gyromagnetic factor and B is the modulus of the field. We consider a field nominally made of a static component along z and a rotating one on the xy plane. Possible imperfections are considered, which may concern the orientation of the static field and some degree of ellipticity in the polarization of the time-dependent terms. Namely, we consider

$$\vec{B} = B\hat{u}_B =$$
$$= B_0\big(\cos(\omega t) + m_1, (1+\varepsilon)\sin(\omega t + \phi) + m_2, m_3\big) \tag{2}$$

with m_1, m_2 accounting for terms that make the static field not perpendicular to the polarization plane xy, and ε, ϕ to describe imperfections of the time-dependent field polarization. B_0 is the nominal amplitude of the rotating field and $m_3 B_0$ is the nominal amplitude of the static one.

The aim is to obtain a time dependent field with a circular polarization on a plane perpendicular to the static term, i.e. the achiemement of $m_1 = m_2 = \varepsilon = \phi = 0$ condition (see eq.(2)).

As known, in the hypothesis of adiabatic following, the macroscopic magnetization $\vec{M}$ maintains a constant modulus M (apart from the decay due to the relaxation mechanisms) while precessing around $\vec{B}(t)$.

Among the components of $\vec{M}$, the one parallel to $\vec{B}$ remains approximately constant, while the perpendicular ones oscillate at high frequency, whose instantaneous value is $\gamma|B|$.

Therefore, neglecting the fast oscillating terms, the dynamics of $\vec{M}$ is determined by the evolution of

$$\vec{M}_\parallel = M_\parallel \hat{u}_B$$

where $M_\parallel$ is constant. The x component of $\vec{M}_\parallel$, that is the low-frequency term revealed by our polarimetric detector and used for dynamic coil calibration is

$$M_{\parallel x}(t) = M_\parallel \frac{B_0\big(m_1 + \cos(\omega t)\big)}{B}. \tag{3}$$

The developed procedure is made of a first step aimed to make $m_1 = m_2 = 0$, and a second one to make $\varepsilon = \phi = 0$. Both the scopes can be pursued on the basis of Fourier analysis of the Taylor approximation of the quantity $M_{\parallel x}(t)$ (eq.(3)), for which the relevant details are reported in the Appendix.

A. Alignment of the static field along z

A straightforward procedure to orient the static field along z is based on minimizing of the Larmor frequency by varying the currents that drive the x and y coils (in the absence of time-dependent fields): the minimum is achieved when the x and y components of the field are fully compensated.

In the presence of a rotating field on the xy plane, a harmonic analysis of the detected signal (eq.(A.1)) can be used to reveal the presence of spurious static components on the xy plane, as well.

Let's analyze the harmonic content of the measured signal described by eq.(3). The power ratio between the second-harmonic terms and the fundamental one (eqs.(A.3) and (A.2)) is:

$$A_2 = \frac{\langle f_2 \rangle^2}{\langle f_1 \rangle^2} = \frac{m_1^2 + m_2^2}{8\left(1 + m_3^2\right)^2}, \tag{4}$$

so that minimizing A_2 will lead to the condition $m_1 = m_2 = 0$, i.e. to a static field perpendicular to the polarization plane of the time-dependent components.

The coefficients m_i represent the ratio between the static field and the rotating one. As the latter must be strong enough to fulfill the adiabatic condition (eq.(1)), A_2 will be typically small. This can make the method not competitive with the one based on the Larmor frequency minimization.

If the static and the time-dependent field components are generated by different coil sets, misalignments might exist between the xy plane defined by the coils that control the static field and the polarization plane of the time-dependent field. As a consequence, the static field can be made perpendicular either to the xy plane or to the polarization plane. The procedure based on Larmor frequency minimization refers to the former, while the one based on harmonic analysis refers to the latter. The study of coil misalignments goes beyond the scopes of this paper, however we note that the just mentioned feature suggests that using the two methods could help highlight such alignment imperfections.

As shown in the Appendix, non-zero values of ϕ and ε do not contribute to second harmonic terms, making the described procedure robust with respect to imperfect polarization of the rotating field. Indeed (see eqs. (A.3) and (A.4)), the polarization imperfections parametrized by ϕ and ε produce only odd harmonic terms, as discussed in the next.

B. Refinement of the field circular polarization on the xy plane

Let's assume that the static field (if any) has been aligned along z, i.e. let the condition $m_1 = m_2 = 0$ and a generic m_3 be achieved. Now, harmonics of the fundamental tone are only ascribed to polarization imperfections, which, as shown in the Appendix, contribute only to odd harmonics of the detected signal.

Making reference to eqs.(A.2) and (A.4), we may derive the power ratio between the third harmonic terms and the fundamental one, finding

$$A_3 = \frac{\langle f_3 \rangle^2}{\langle f_1 \rangle^2} = \frac{\varepsilon^2 + \phi^2}{32 \left(1 + m_3^2\right)^2}, \qquad (5)$$

similarly to the case of eq.(4), minimizing A_3 will lead toward the $\varepsilon = \phi = 0$ condition, i.e. to a condition of perfectly circular polarization of the time dependent field.

It is worth examining possible consequences of imperfect perpendicularity of the static field on the accuracy of this procedure. In fact, beside the analyzed second-harmonic terms, a non perpendicular static field causes also third-harmonic signal, mimicking polarization issues. However, as shown in eq.(A.4), m_1 and m_2 in a first-order Taylor approximation do not produce such terms, and they only contribute when also the second order (eq.(A.5)) is taken into account. In this sense, the procedure aimed to obtain circular polarization is robust with respect to the $m_1 = m_2 = 0$ requirement.

IV. VALIDATION

In this section we report experimental results validating the proposed methodology. We first investigate the effects of static field misalignments (analyzed in Sec.III A) and then those of imperfect polarization (analyzed in Sec.III B).

A. Effects of static field misalignment

We have performed a measurement having aligned the field along z on the basis of Larmor frequency minimization in the absence of any rotating field. The static field inferred from the free precession is about 1 μT. We have then applied a field of 16 μT rotating at 3144 Hz, thus the nominal condition is $m_1 = m_2 = 0$, $m_3 = 1/16$, the relative phase of the oscillating x, y components is set to $\pi/2$ on the basis of the static calibration factor. The recorded signal is reported in Fig.3: no second harmonic peak appear, while a weak third harmonic peak is visible, about 33 dB below the fundamental tone. We have then applied an additional transverse static component that shifts the free precession frequency to 4950 Hz: this corresponds to have $(m_1, m_2, m_3) \approx (0, 52, 66) \cdot 10^{-3}$, which according to eq.(4) causes a second harmonic peak about 34 dB below the fundamental tone. This expectation is in perfect accordance with the signal analysis shown in Fig.4.

Noticeably, the measurements shown in Figs.3 and 4 put in evidence also an increase of the decay time with respect to the case of free precession around a static field (Fig.2). Such increase is due to mechanisms emerging when the spin dynamics is driven by a rotating fields much stronger than the static one. These mechanisms are currently under investigation and this phenomenon is not further discussed in this work.

B. Effects of polarization ellipticity

Rotating fields with variable degree of ellipticity are applied to compare theoretical and experimental evaluations of $A_3(\varepsilon, \phi)$. In the experiments, the couple (ε, ϕ) is varied around its nominal $(0,0)$ value estimated on the basis of static calibration factors. Discrepancies between static and dynamic calibration factors appear as a translation of the surface $A_3(\varepsilon, \phi)$, in particular as a displacement of its minimum.

The plots in Fig.5 shows a 3D representation of calculated $A_3(\varepsilon, \phi)$ and corresponding experimental results obtained $m_1 = m_2 = 0$ (set by minimizing the Larmor frequency in the initial presence of $m_3 \neq 0$) and with $m_3 \approx 0$ having minimized the second harmonic peak.
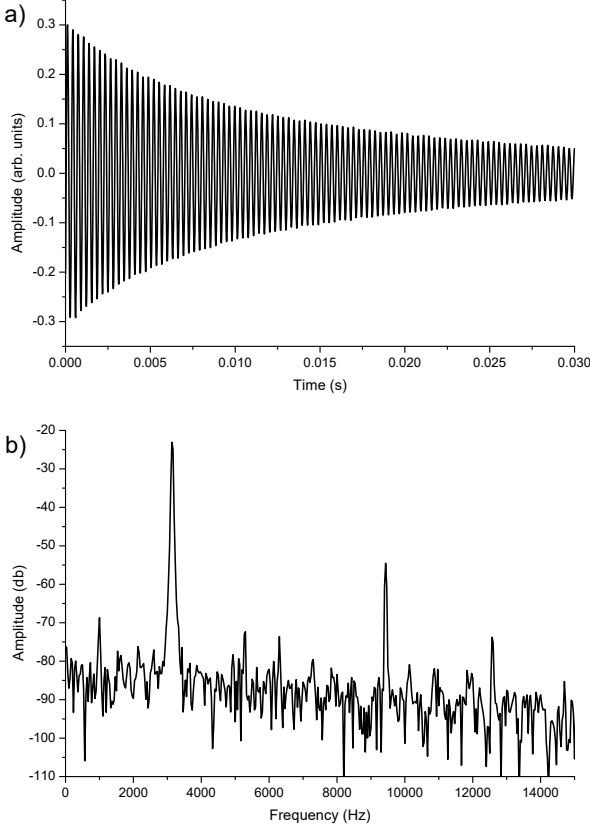
FIG. 3. Signal generated from atomic magnetization adiabatic following a 16 μT field rotating at 3.144 kHz on the xy plane, while the static field is the same as for Fig.2, in time (a) and frequency (b) domain, respectively. A second harmonic peak is barely visible, about 45 dB below the fundamental tone.

The measurements have been performed with $\omega = 2\pi \cdot 1474$ rad/s, under the application of a rotating field deliberately distorted with the application of variable couples (ε, ϕ) in the range $[-0.15, +0.15] \times [-0.15 \text{ rad}, +0.15 \text{ rad}]$. The matching is substantial, both in the surface shape and in the absolute values: the minor deviation (about 13%) of the latter is due to a low-pass filtering effect by the transimpedance amplifier of the photodetector.

The same data are then shown as 2D plots in Figs.6a and 6b, in which a displacement of the minimum is barely detectable: $(\varepsilon_{\mathrm{MIN}}, \phi_{\mathrm{MIN}}) = (8 \cdot 10^{-4}, 0.35°)$. Such displacement of the minimum is ascribed to the ellipticity that is obtained when the static calibration factors are used to produce alternating fields.

Higher frequencies of the rotating field cause larger discrepancies from the static calibration, which results in larger displacement of the minimum. The map in Fig.6c is obtained with a 30 μT field rotating at 4950 Hz. In this case, the minimum of the A_3 ratio is located in $(\varepsilon_{\mathrm{MIN}}, \phi_{\mathrm{MIN}}) = (0.0195, -1.7°)$
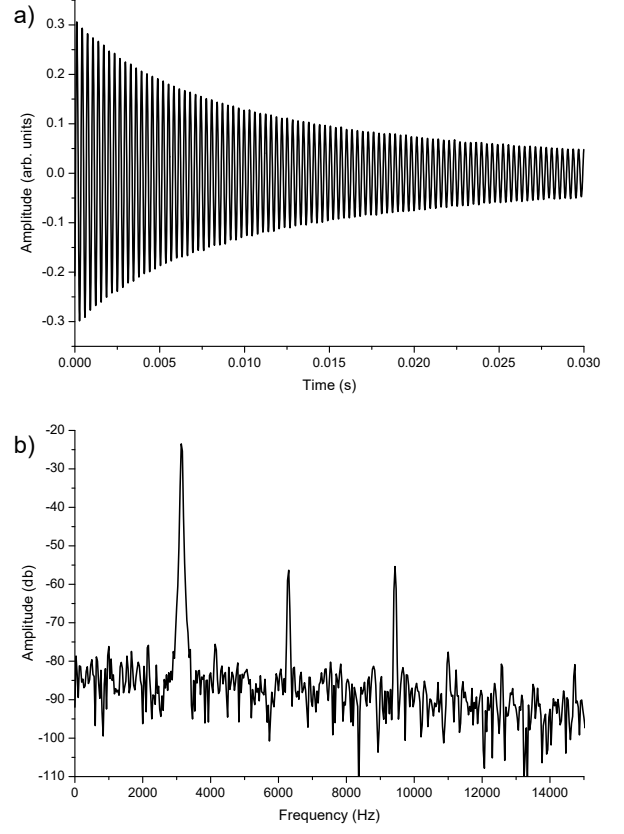
The experimental maps confirm the theoretical predic-

FIG. 4. As in Fig.3, the magnetization adiabatically follows a 16 μT, 3.144 kHz field rotating on the xy plane. But a transverse component (830 nT in amplitude) is added to the static field along the z direction. Also in this case the signal is plotted in the time (a) and frequency (b) domains. Compared to Fig.3b a clear emergence of a second-harmonic peak occurs. That peak is here about 34 dB below the fundamental tone, in accordance with the prediction of eq.(4).

tion, and appear with the expected convex surface over wide intervals of the parameters. This suggests that optimization algorithms can be reliably implemented in the experiments to adjust the relative amplitude and phase of the rotating field in order to refine the calibration and to eventually generate a circular polarization at a given frequency.

More generally, the method can be applied to identify the actual phase difference between the drive signal and the magnetic field generated by each coil, i.e. to obtain accurate calibration factors for operating at frequencies where the static calibration are not applicable.

V.   CONCLUSION

We have presented an innovative methodology to align static components of a magnetic field and to calibrate its time-dependent components on the basis of *in-situ* measurements performed with a setup for optical-pumping
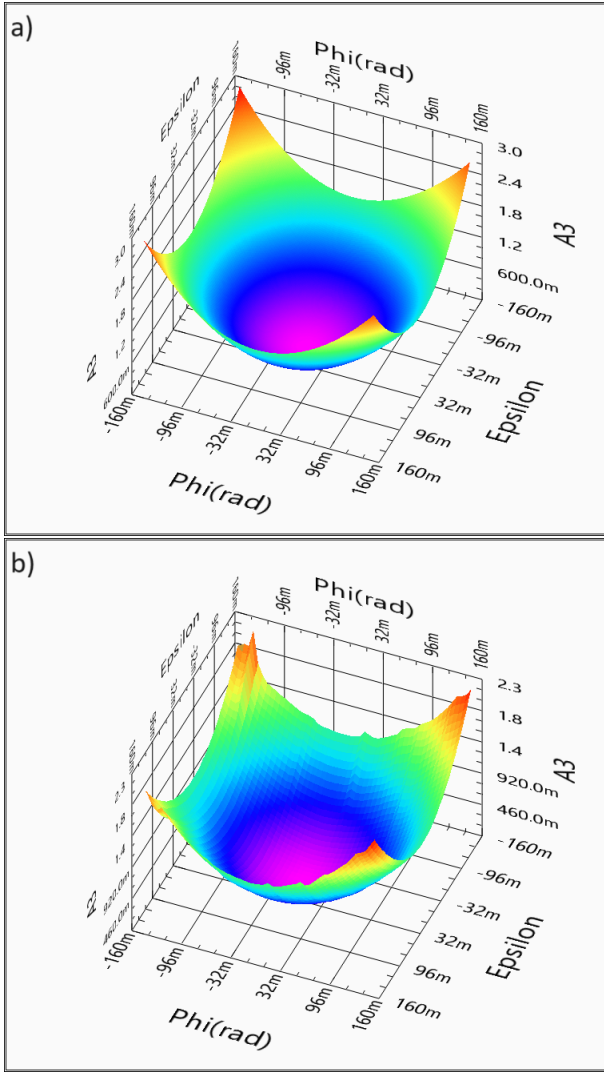
FIG. 5. Comparison between calculated (a) and experimental (b) 2D maps for both ε and ϕ spanning a $[-0.15, 0.15]$ range. The experimental one is obtained with 50×50 measurements of A_3, with a low-frequency (1474 Hz) rotating field 16 μT in amplitude.

magnetometry.

The developed procedures are based on the harmonic analysis of polarimetric signals recorded in the presence of an intense, rotating magnetic field and, possibly, of a static one.

We have shown that second harmonic terms can be used to align the static field perpendicularly to the polarization plane of the rotating one. Then we have described a procedure suited to refine the circular polarization of the latter. In typical conditions, the first goal can be better achieved with a traditional approach based on Larmor frequency minimization. In contrast, the method developed to the second end constitutes a very useful tool when relative amplitudes and phases of fast oscillating field components must be precisely assigned.

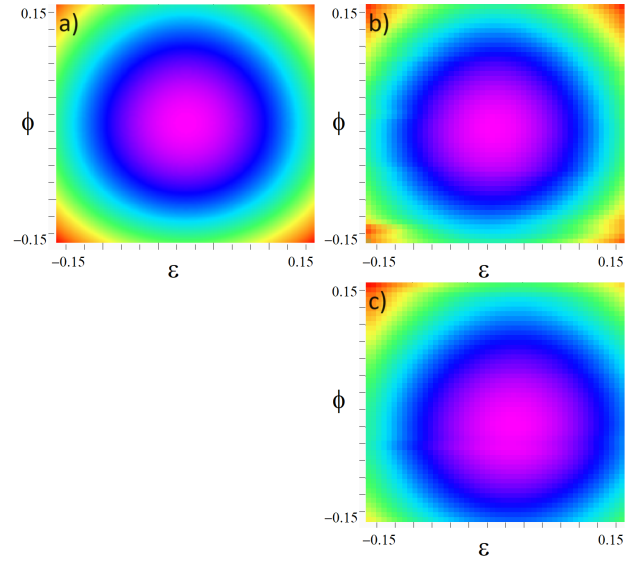We have developed and examined the procedure to pro-

FIG. 6. The theoretical and experimental data reported in Fig.5 are here represented in the 2D maps a) and b), respectively. The map c) is recorded with a 30 μT field rotating at a higher frequency (4950 Hz). As expected, the higher frequency causes a larger shift of the observed minimum with respect the central point of the map, which corresponds to $(\varepsilon, \phi) = (0, 0)$ on the basis of the static calibration. The displacement of the recorded minimum is $(8 \cdot 10^{-4}, 0.35°)$ in case b) and $(0.0195, -1.7°)$ in case c).

duce a circularly polarized field on a given plane. Analogous procedures can be implemented on an perpendicular plane and at the diverse frequencies of interest. This would provide a complete set of calibration factors, sufficient to generate three-dimensional fields with arbitrary time-dependence.

APPENDIX

As discussed in Sec.III, the proposed methodology (developed to point out spurious components of the static field and polarization imperfections of the time-dependent one) is based on the harmonic analysis of the detected signal, which is proportional to the x component of $\hat{u}_b(t) = \vec{B}(t)/B(t)$ that is

$$S(t) = (m_1 + \cos(\omega t))[(m_1 + \cos(\omega t))^2 + \\ + (m_2 + (1 + \varepsilon)\sin(\omega t + \phi))^2 + m_3^2]^{-1/2} \quad \text{(A.1)}$$

A Taylor expansion of $S(t)$ followed by a Fourier analysis leads to determine the signal components at ω and its multiples. As explained in Sec.III, harmonic terms evidence misalignments of the static field and imperfections of the polarization of the time-dependent field.

It is convenient to normalize the harmonics terms to the fundamental one, to cancel the effects of spurious amplitude fluctuations of $S(t)$ that may occur, e.g., due

to fluctuations in the power or in the tuning of the laser sources. Thus we evaluate here in a first order Taylor approximation the terms at ω, 2ω and 3ω, which are relevant to the proposed analysis.

The fundamental tone is:

$$f_1 = \frac{\cos(\omega t)}{\left(1 + m_3^2\right)^{1/2}} - \frac{\varepsilon \cos(\omega t) + \phi \sin(\omega t)}{4\left(1 + m_3^2\right)^{3/2}}; \qquad \text{(A.2)}$$

the first-order terms oscillating at 2ω only depend on m_1 and m_2:

$$f_2 = -\frac{m_1 \cos(2\omega t) + m_2 \sin(2\omega t)}{2\left(1 + m_3^2\right)^{3/2}}, \qquad \text{(A.3)}$$

while the third-harmonic ones are expressed by

$$f_3 = \frac{\varepsilon \cos(3\omega t) - \phi \sin(3\omega t)}{4\left(1 + m_3^2\right)^{3/2}}, \qquad \text{(A.4)}$$

with no dependence on m_1, m_2: the misalignment terms contribute to the third harmonics only at the second order term, which reads

$$f_{3-2nd} = \frac{\alpha \cos(3\omega t) + \beta \sin(3\omega t)}{32\left(1 + m_3^2\right)^{5/2}}, \qquad \text{(A.5)}$$

with $\alpha = (4m_3^2 - 5)\varepsilon^2 - (8m_3^2 + 11)\phi^2 + 12(m_1^2 - m_2^2)$ and $\beta = (16m_3^2 + 10)\varepsilon\phi - 24m_1 m_2$.

[1] T. Wang, W. Lee, M. Romalis, M. Limes, T. Kornack, and E. Foley, Pulsed ^{87}Rb vector magnetometer using a fast rotating field (2023), arXiv:2304.00214 [quant-ph].

[2] A. J. Fallon, S. J. Berl, E. R. Moan, and C. A. Sackett, Precise control of magnetic fields and optical polarization in a time-orbiting potential trap, Phys. Rev. A **102**, 023108 (2020).

[3] J. Tajuelo, O. Martínez-Cano, J. R. Morillas, J. Yang, and J. de Vicente, Generation of synchronized high-frequency triaxial magnetic fields using fractal capacitor banks, Phys. Rev. Appl. **20**, 044063 (2023).

[4] N. Holmes, T. M. Tierney, J. Leggett, E. Boto, S. Mellor, G. Roberts, R. M. Hill, V. Shah, G. R. Barnes, M. J. Brookes, and R. Bowtell, Balanced, bi-planar magnetic field and field gradient coils for field compensation in wearable magnetoencephalography, Scientific Reports **9**, 14196 (2019).

[5] V. Gerginov, Field-polarization sensitivity in rf atomic magnetometers, Phys. Rev. Appl. **11**, 024008 (2019).

[6] G. Bevilacqua, V. Biancalana, A. Vigilante, T. Zanon-Willette, and E. Arimondo, Harmonic fine tuning and triaxial spatial anisotropy of dressed atomic spins, Phys. Rev. Lett. **125**, 093203 (2020).

[7] J. Humar, D. Fefer, and G. Geršak, AC/DC transfer method for an AC magnetic flux density standard, Measurement Science and Technology **16**, 1656 (2005).

[8] K. Weyand, R. Ketzler, and M. Kitschke, Calibration of magnetic field coil standards by means of field profile measurement, International Journal of Applied Electromagnetics and Mechanics **22**, 169 (2005).

[9] E. Breschi, Z. Grujić, and A. Weis, In situ calibration of magnetic field coils using free-induction decay of atomic alignment, Applied Physics B **115**, 85 (2014).

[10] H. Zhang, S. Zou, and X.-Y. Chen, A method for calibrating coil constants by using an atomic spin co-magnetometer, The European Physical Journal D **70**, 203 (2016).

[11] H. Yao, D. Ma, J. Zhao, J. Lu, and M. Ding, A coil constant calibration method based on the phase-frequency response of alkali atomic magnetometer, Photonic Sensors **9**, 189 (2019).

[12] L. Chen, B. Zhou, G. Lei, W. Wu, J. Wang, Y. Zhai, Z. Wang, and J. Fang, A method for calibrating coil constants by using the free induction decay of noble gases, AIP Advances **7**, 075315 (2017).

[13] Q. Zhao, B. Fan, S. Wang, and L. Wang, A calibration method for coil constants using an atomic spin self-sustaining vector magnetometer, Journal of Magnetism and Magnetic Materials **514**, 166977 (2020).

[14] G. Zhang, S. Huang, and Q. Lin, In situ calibration of magnetic coil system using ellipticity-induced Bell-Bloom magnetometer, IEEE Photonics Journal **11**, 1 (2019).

[15] K. Wang, D. Ma, S. Li, Y. Ma, Y. Gao, Y. Dou, and J. Sun, Triaxial coils in situ calibration method based on measuring the alternating magnetic field-induced dynamic response of the SERF magnetometer, IEEE Sensors Journal **23**, 18099 (2023).

[16] K. Zhang, M. Cao, J. He, W. Gong, and Y. Huang, An alternating current calibration method for Helmholtz coil constant based on orthogonal calculation principle, Metrology and Measurement Systems **vol. 30**, 549 (2023).

[17] G. Bevilacqua, V. Biancalana, T. Zanon-Willette, and E. Arimondo, Harmonic dual dressing of spin-1/2 systems, Phys. Rev. A **105**, 022619 (2022).

[18] A. Fregosi, C. Marinelli, C. Gabbanini, G. Bevilacqua, V. Biancalana, E. Arimondo, and A. Fioretti, Floquet space exploration for the dual-dressing of a qubit, Scientific Reports **13**, 15304 (2023).

[19] G. Bevilacqua, V. Biancalana, Y. Dancheva, A. Fregosi, G. Napoli, and A. Vigilante, Electromagnetic induction imaging: signal detection based on tuned-dressed optical magnetometry, Opt. Express **29**, 37081 (2021).

[20] S. Haroche, C. Cohen-Tannoudji, C. Audoin, and J. P. Schermann, Modified Zeeman hyperfine spectra observed in h^1 and rb^{87} ground states interacting with a nonresonant rf field, Phys. Rev. Lett. **24**, 861 (1970).

[21] G. Bevilacqua, V. Biancalana, Y. Dancheva, and L. Moi, Larmor frequency dressing by a nonharmonic transverse magnetic field, Phys. Rev. A **85**, 042510 (2012).

[22] G. Bevilacqua, V. Biancalana, P. Chessa, and Y. Dancheva, Multichannel optical atomic magnetometer operating in unshielded environment, Applied Physics B **122**, 103 (2016).

[23] V. Biancalana, G. Bevilacqua, P. Chessa, Y. Dancheva, R. Cecchi, and L. Stiaccini, A low noise modular current source for stable magnetic field control, Review of Scientific Instruments **88**, 035107 (2017), http://dx.doi.org/10.1063/1.4977931.

[24] L. Lenci, S. Barreiro, P. Valente, H. Failache, and A. Lezama, A magnetometer suitable for measurement of the Earth's field based on transient atomic response, Journal of Physics B: Atomic, Molecular and Optical Physics **45**, 215401 (2012).

[25] Z. D. Grujić, P. A. Koss, G. Bison, and A. Weis, A sensitive and accurate atomic magnetometer based on free spin precession, The European Physical Journal D **69**, 135 (2015).